International Journal of Thin Films Science and Technology

http://dx.doi.org/10.12785/ijtfst/040101

Influence of Post Thermal Annealing on the Optical Properties of SnO_2 Films Prepared by Electron Beam Evaporation Technique.

H. A. Mohamed[*,1,2] *and N. M. A. Hadia*[2]

[1]Physics department, Faculty of Science, Sohag University, 82524 Sohag, Egypt
[2]Physics department, Teachers College, King Saud University, 11148 Riyadh, KSA.

Received: 7 Jun. 2014, Revised: 21 Sep. 2014, Accepted: 23 Sep. 2014.
Published online: 1 Jan. 2015.

Abstract: This work reports on the effect of post thermal annealing on the optical properties of SnO_2 films. The films were deposited using electron beam evaporation technique. The films were annealed in air in the temperature range 200-550 ^oC. It was found that the annealing temperature has a significant effect on the optical properties of these films. The films are transparent in the visible region with average transmission of 83%. A high optical energy-gap of 3.65 eV was achieved at temperature 500 ^oC. Many optical parameters such as: refractive index; extinction coefficient; degree of inhomogeneity; dielectric constants; single oscillator energy; dispersion energy; oscillator strength; average oscillator wavelength; static dielectric constant; high frequency dielectric constant; thermal emissivity and optical resistivity were calculated as a function of annealing temperature. Finally, SnO_2 films can be used in transparent heat mirror coatings applications due to their low thermal emissivity at high annealing temperature.

Keywords: SnO_2, TCO thin film, electron beam, post thermal annealing, optical properties. PACS number: 78.66. ± w, 78.20.Ci, 81.15. ± z.

1 Introduction

Transparent conductive oxides (TCOs) films are unusual materials that are both electrically conductive (electrical resistivity ~ 10-4 Ω cm) and visually transparent (visible transmittance >80%). These transparent, metallic oxides include, in part, indium oxide, tin oxide, indium tin oxide, zinc oxide, and cadmium tin oxide. Although partial transparency, with acceptable reduction in conductivity, can be obtained for very thin metallic films, high transparency and simultaneously high conductivity cannot be obtained in intrinsic stoichiometric materials. The only way this can be achieved is by creating electron degeneracy in a wide band gap (Eg > 3.5 eV or more for visible radiation) material by introducing nonstoichiometry and/or appropriate dopants in a controlled manner.

These conditions can be conveniently met for ITO as well as a number of other materials [1]. TCO are currently of great commercial importance for applications in transparent electrodes for flat panel displays, solar cells, organic light emitting diodes, electrochromics, and low-emissivity window [2-5]. SnO2 is n-type semiconducting oxide with wide band gap (Eg = 3.6 eV at 300 K) and is grown as tetragonal crystal structures [6,7]. SnO_2 thin films have low resistivity and high optical transparency in the visible region of electromagnetic spectrum. SnO_2 thin films have some advantage in contrast to other TCO films that contain expensive, scarcity and toxic elements (In, Ti, Cd etc.). SnO_2 has better thermal resistance than indium tin oxide (ITO), its films are relatively hard and they have good abrasion and scratch resistance [8]. High hardness of SnO_2 films is important for application of transparent conductive films as protective layers on soft and transparent substrates, such as polymer materials for vehicular and aircraft canopies, windows and windshields [9]. Thus, the properties of SnO_2 and its relatively low cost, make it preferable in some applications requiring a conducting layer on glass.

Thin films of SnO_2 can be prepared by many techniques, such as chemical vapor deposition [10], sputtering [11], sol-gel [12], reactive evaporation [13], pulsed laser ablation [14], screen printing technique [15], spray pyrolysis [16], SILAR [17] and electron beam evaporation [18]. In this work, SnO_2 films were deposited onto microscopic glass substrates by electron beam evaporation method. The effects of post thermal annealing on the optical properties, such as transmission, reflectance, energy-gap, refractive index, extinction coefficient, degree of inhomogeneity, dielectric constant, oscillator strength, average oscillator wavelength, static dielectric constant, high frequency dielectric constant, thermal emissivity and optical resistivity, were investigated.

*Corresponding author e-mail: hussein_abdelhafez2000@yahoo.com

2 Experimental Section

Tablets from highly pure (99.999) SnO_2 were formed using a cold pressing. Edward's high vacuum coating unit model E306A under pressure of 5×10^{-5} Torr during film deposition was used to prepare SnO_2 films onto ultrasonically cleaned glass slides of dimension 2.5 × 1 cm. The film thickness (~100 nm) and deposition rate were controlled by means of a digital film thickness monitor model TM200 Maxtek. The transmittance (T) and reflectance (R) data were measured using a Jasco V-570 ultraviolet-visible-near infrared (UV-VIS-NIR) spectrophotometer in the wavelength range from 200 to 2500 nm at normal incidence. The heat treatment (annealing temperature) has been performed in air at different temperatures from 200 to 550 ◦C for fixed time of 60 min using a fully controlled furnace (model Lindberg). The optical parameters, namely optical energy-gap (E_g), free carrier concentration (N), refractive index (n), extinction coefficient (k), real and imaginary dielectric constants (ε', ε''), optical resistivity (ρ_{opt}), single oscillator energy (E_0) and a dispersion energy (E_d) were calculated using the two aforementioned quantities (T and R).

3 Results and Discussion

Transmittance spectra observed of as-deposited and after heat treatment of SnO_2 films are presented in Fig. 1. It is observed that the as-deposited films represent low transmission value and the thermal annealing at low temperature has not significant effect. At annealing temperature of 400 ^oC, small increase in transmission spectrum is observed particularly at near-infrared region (NIR). This behavior of transmission for as-deposited films and at low value of annealing temperature is expected for TCO films that deposited by electron beam technique due to oxygen deficiency resulting during the electron beam evaporation process [19, 20]. The films that annealed at 450 ^oC show transmission of 68% in the visible region indicating that annealing process in air at this temperature is suitable to substitute the reduction in oxygen. With further increase in annealing temperature, the transmission increases up to 83% at temperature of 500 ^oC. The films annealed at 550°C shows a small decrease in visible light transmittance. It may be attributed to the light scattering effect for its higher surface roughness [21]. Fig.2 shows the reflectance spectra of SnO_2 films annealed at different temperatures. It is clear that the as-deposited films and films annealed at low temperature up to 400 ^oC have the same behavior, where high value (> 50%) of reflectance was observed at NIR region indicating that these films have high value of free carrier concentrations.

While the films that annealed at high temperature 450-550 ^oC have different behavior and their reflectance are small comparing with the above films.

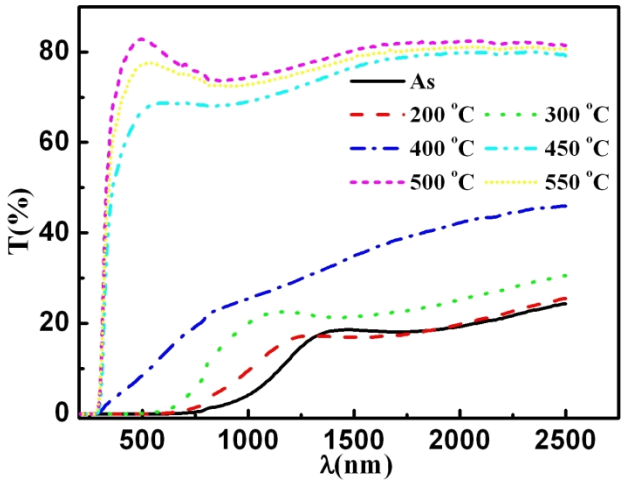

Fig.1 The optical transmittance spectra of the SnO_2 films as a function of the annealing temperature.

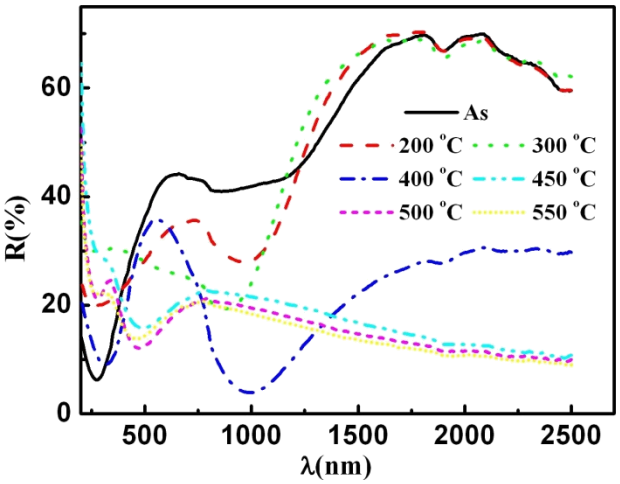

Fig.2 The optical reflectance spectra of the SnO_2 films as a function of the annealing temperature.

Using the measured values of transmission (T) and reflection (R), the absorption coefficient α can be written in the form [21]:

$$\alpha = \frac{2.303}{d} log_{10}\left(\frac{1-R}{T}\right) \quad (1)$$

Where d is the film thickness.

The absorption coefficient can be used to determine the optical band gap E_g following equation:

$$\alpha h\nu = A\left(h\nu - E_g\right)^n \quad (2)$$

Where A is a constant, $h\nu$ is the photon energy and the exponent, $n=1/2$ for allowed direct, $n=2$ for allowed indirect, $n=3/2$ for forbidden direct and $n=3$ for forbidden indirect transitions. The present work shows that SnO_2 films have direct allowed transition as shown in Fig.3-a. The variation of estimated E_g with annealing temperature is shown in Fig.3-b.

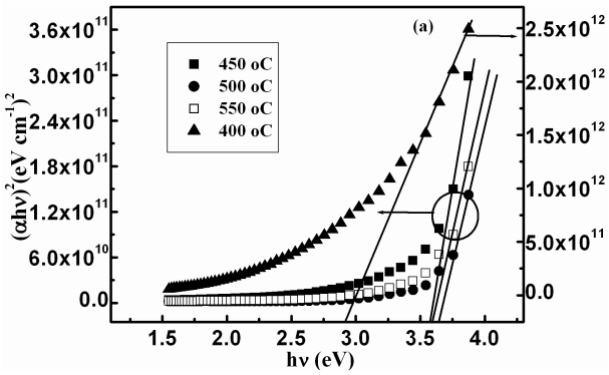

(a)

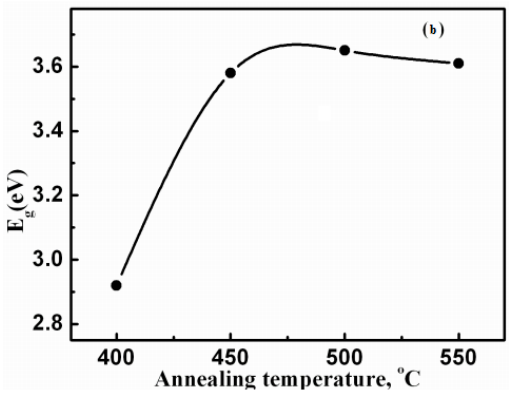

(b)

Fig.3: The $(\alpha hv)^2$ vs. photon energy (hv) plot of the SnO_2films annealed at different temperatures (a) and the estimated direct allowed optical energy-gap at different temperatures, ranging from 400 to 550 ^oC (b).

Due to the poor transmittance and undistinguishable absorption edge, the E_g of as-deposited films and the annealed film at low annealing temperature (< 400 ^oC) could not be estimated. The E_g of the films annealed at 400 ^oC is 2.92 eV, which is increased to 3.65 eV when annealed at 500 ^oC but then decreased with the further increase in annealing temperature to reach 3.61 eV at temperature of 550 ^oC. Optical parameters namely, refractive index (n) and extinction coefficient (k), have been determined from the transmittance (T) and reflectance (R) measurements using Taus model [23]:

$$n = \frac{1+R}{1-R} \pm \left[\left(\frac{1+R}{1-R}\right)^2 - (1+k^2)\right]^{1/2} \quad (3)$$

$$K = \frac{2.303\lambda}{4\pi d} log_{10}\left(\frac{1-R}{T}\right) \quad (4)$$

The average refractive index and extinction coefficient in the wavelength range 400-800 nm is calculated using the above equations and plotted in Fig.4 as a function of annealing temperature. It is seen that both the refractive index as well as the extinction coefficient of the SnO_2 films are decreased as a result of annealing. The decrease in extinction coefficient with annealing can be correlated to the decrease of absorption (increase in transmission) with increasing the temperature of annealing as seen from Eq. (4) and Fig.1. The behavior of refractive index can be understood in terms of the behavior of energy-gap. The refractive index of the films is calculated using Moss relation [23,24] which is directly related to the fundamental energy-gap (E_g),

$$E_g = \frac{A}{n^4} \quad (5)$$

Where A is a constant with a value of 108 eV. A different relation between the refractive index and bangap energy is presented by Herve and Vandamme in the following for [25],

$$n = \sqrt{1 + \left(\frac{B}{E_g + C}\right)^2} \quad (5)$$

Where B and C are numerical constants with values of 13.6 and 3.4 eV, respectively. The changing of refractive index (n) with annealing temperature is shown in Table 1 for these three models (Taus, Moss, Herve and Vandamme). As seen from the table 1, the refractive index values decrease with increasing annealing temperature and the rate of increase seems to be dependent on the used models. Where, the refractive index calculated by Taus model is closed to this calculated by Moss model particular at high temperature.

Table 1: The bandgap (E_g), refractive index (n), optical static dielectric constant (ϵ_0) and optical high frequency dielectric constant (ϵ_i) values of SnO_2 thin films as a function of annealed temperature.

T(°C)	E_g(eV)	ϵ_0	Taus model		Moss relation		Herve &Vandamme	
			n	ϵ_i	n	ϵ_i	n	ϵ_i
400	2.92	9.52	3.2	10.2	2.45	6	2.37	5.6
450	3.58	7.49	2.55	6.5	2.34	5.5	2.19	4.8
500	3.65	7.28	2.38	5.7	2.33	5.4	2.17	4.7
550	3.61	7.4	2.43	5.9	2.33	5.4	2.18	4.75

Moreover, the decrease in refractive index with increasing annealing temperature can be attributed to the increase of the degree of homogeneity of SnO_2 films with increasing annealing. It is known that a high percentage of voids exist in the oxide thin films, especially in the surface layer of the thin films and this percentage is gradually decrease with annealing process [26]. The degree of inhomogeneity of SnO_2 films can be expressed by $\Delta n/n$, where Δn and n refer to variation and average values of the refractive index measured at wavelengths in the range of 400–800 nm. The

degree of inhomogeneity as a function of annealing temperature is plotted in Fig.5.

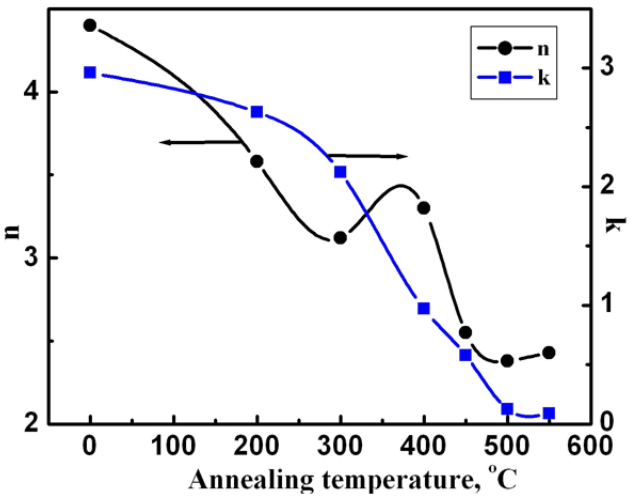

Fig.4 The refractive index (n) and extinction coefficient (k) of SnO_2 films at different annealing temperatures.

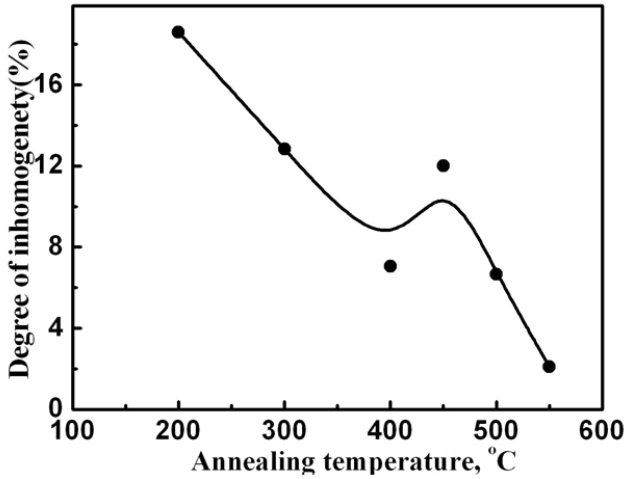

Fig.5 Degree of inhomoginity as a function of annealing temperature of SnO_2 films.

The dispersion behavior, as we all know, plays an important role in the research for optical materials, because it is a significant factor in optical communication and designing of the devices for spectral dispersion. The single-oscillator Wemple–DiDomenico (W–D) dispersion model is used to analyze experimental data of refractive index, which usually provides physically significant quantities such as the oscillator energy in the interband transition region. The W–D dispersion model can be described as [27]:

$$n^2 - 1 = \frac{E_0 - E_d}{E_0^2 - E^2} \quad (7)$$

Where E is the photon energy, E_0 is the single-oscillator energy, E_d is the dispersion energy, which is a measure of the intensity of the interband optical transitions. The curves of $(n^2 -1)^{-1}$ versus E^2 for the SnO_2 films are plotted in Fig. (6-a) and the data are fitted into straight lines, indicating the W–D dispersion model is applicable to the SnO_2 films in the present work. The values of E_0 and E_d can be determined from the slope $(1/E_0E_d)$ and intercept (E_0/E_d) on the vertical axis and are plotted in Fig.(6-b) as a function of annealing temperature. It is clear that E_0 increases with increasing annealing temperature and has the same behaviour of energy-gap [27] as shown in Fig.(3-b). While, E_d increases with increasing annealing temperature up to 300°C and then start to decrease with further increase in temperature. The dispersion data of the refractive index can also be analyzed using Sellmeir dispersion formula [28] that is given by:

$$n^2 - 1 = \frac{\lambda_0^2 - S_0}{1 - \left(\lambda_0/\lambda\right)^2} \quad (8)$$

Where λ is the wavelength of incident light, λ_0 is the average oscillator wavelength and S_0 is the oscillator strength. Fig.(7-a) shows the relation between $(n^2 -1)^{-1}$ versus $1/\lambda^2$ for the SnO_2 films. The values of S_0 and λ_0 can be estimated from the slope $(1/S_0)$ and the infinite wavelength intercept $(1/S_0\lambda_0^2)$ of the above curves and are plotted in Fig.(7-b) as a function of annealing temperature. It is observed that S_0 decreases with increasing the annealing temperature while λ_0 increases with increasing at low values of temperature and then starts to decrease at high values of temperature.

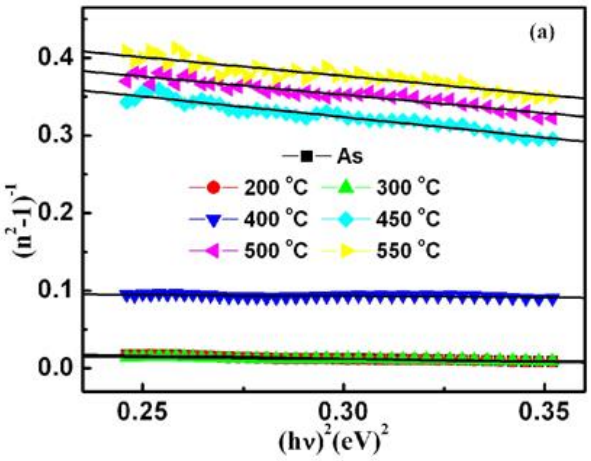

(a)

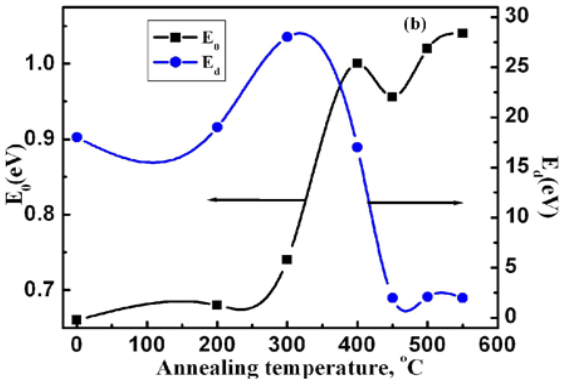

(b)

Fig.6 The $(n^2\text{-}1)^{-1}$ vs. $(hv)^2$ plots of the SnO_2 thin films at different annealing temperatures (a), the variation of oscillator energy (E_0) and dispersion energy (E_d) with annealing temperature (b).

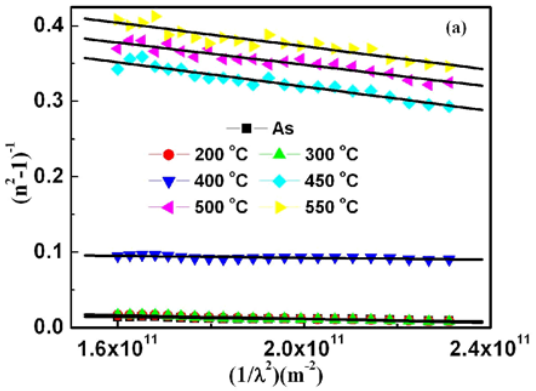

(a)

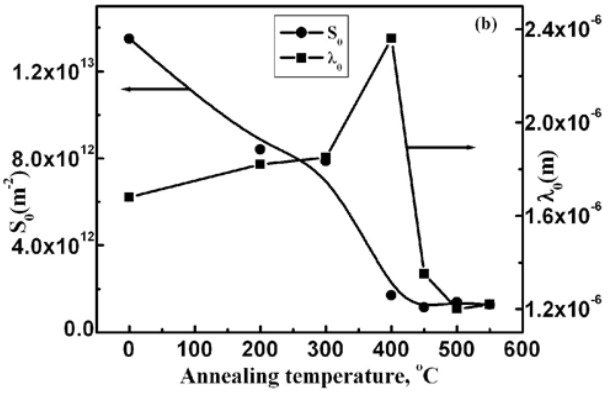

(b)

Fig.7 The $(n^2\text{-}1)^{-1}$ vs. $(1/\lambda^2)$ plots of the SnO_2 thin films at different annealing temperatures (a), the variation of oscillator strength (S_0) and average oscilotor wavelength (λ_0) with annealing temperature (b).

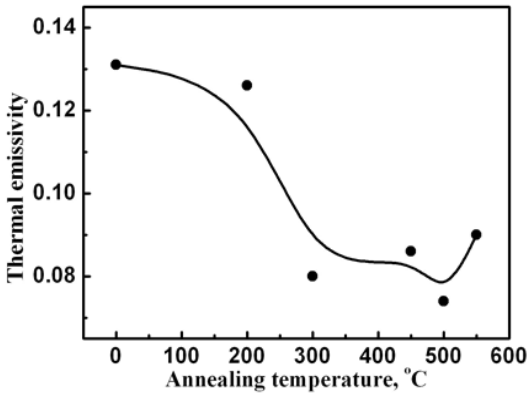

Fig.8 Dependence of thermal emissivity of SnO_2 films on the annealing temperature.

One of valuable applications transparent conducting oxides, transparent heat mirror coatings (low thermal emissivity) have attracted increased interest in reducing heat radiation loss through window panes from ecological and sustainable aspects [29]. The thermal emissivity of SnO_2 can be calculated from the following relation [30]:

$$\varepsilon = 1 - (T_{IR} + R_{IR}) \tag{9}$$

Where T_{IR} and R_{IR} are the average transmission and reflection in the near infrared region (λ=1800-2500 nm), respectively. Fig.8 shows the dependence of thermal emissivity of SnO_2 films on the annealing temperature. It can be noted that the thermal emissivity decreases with increasing annealing temperature and attains its minimum value of 0.07 % at temperature 500 °C. The small increase in thermal emissivity at temperature 550 °C maybe due to decreasing the transmission at this temperature as shown in Fig.1.

The fundamental electron excitation spectrum of the films is described by using a frequency dependence of the complex electronic dielectric constant. The dielectric constant is defined as [21]:

$$\begin{aligned}\varepsilon(\lambda) &= \big(n(\lambda) - ik(\lambda)\big)^2 \\ &= \varepsilon'(\lambda) - i\varepsilon''(\lambda)\end{aligned} \tag{10}$$

Where ε' and ε'' are the real and imaginary dielectric constant, respectively. Using Drude's theory of dielectrics [32], the real dielectric constant (ε') can be written as:

$$\varepsilon' = n^2 - k^2 = \varepsilon_i - \frac{e^2}{4\pi^2 c^2 \varepsilon_0}\left(\frac{N}{m^*}\right)\lambda^2 \tag{11}$$

where ε_i is the infinitely high frequency dielectric constant or the residual dielectric constant due to the ion core, ε_0 is the permittivity of free space, N/m^* is the ratio of carrier concentration to the effective mass, c is the light velocity, λ is the incident light wavelength and e is the elementary charge. The variation of real part of dielectric constant with wavelength is shown in Fig.9 for different values of annealing temperature.

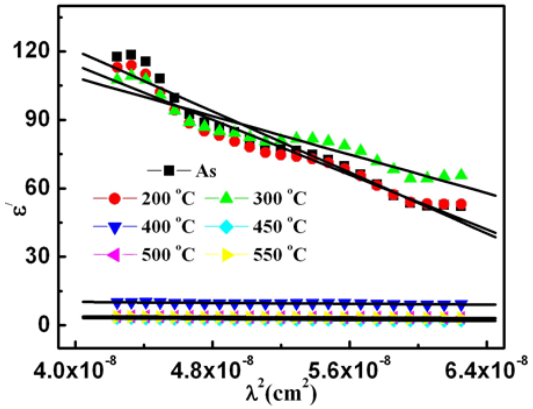

Fig.9 Variation of real part (ϵ') of the dielectric constant of SnO_2 films with λ^2 at different annealing temperatures.

The concentrations of free carrier (N) are calculated from the slope of the above relation and are plotted as a function of annealing temperature as shown in Fig.10. It is clear that N decreases with increasing the annealing temperature which can be attributed to decrease of reflectance with annealing as shown in Fig.2. The dielectric behavior of solids is important for several electrondevice properties. Both static and high frequency dielectric constants were evaluated for all the films. The high frequency dielectric constant (ε_i) and the static dielectric constant (ε_0) of the films are calculated from the following relation [17]:

$$\varepsilon_i = n^2, \varepsilon_0 = 18.52 - 3.08E_g \qquad (12)$$

Where n is the refractive index and E_g is the energy-gap. The estimated values of ε_i and ε_0 *are* listed in table 1 for Taus model, Moss relation and Herve & Vandamme model.

The optical resistivity ρ_{opt} of SnO_2 films is calculated using the following equation [33]:

$$R = 1 - 4\left(\frac{\varepsilon_0 C}{d}\right)\rho_{opt} \qquad (13)$$

Where R, ε_0, C and d are respectively the reflectance in near infrared region, permittivity of free space, light velocity and film thickness. Fig.10 shows the variation of optical resistivity of SnO_2 films with annealing temperature. The increasing of optical resistivity with annealing is observed in this figure. This due to decreasing the reflectance of SnO_2 film in near infrared region with increasing the annealing temperature or/and decreasing the free carrier concentrations. The as-deposited films represent optical resistivity of 3.27×10^{-4} Ω cm, while the values of optical resistivity are in the range of 3.32×10^{-4}-8.5×10^{-4} Ω cm which corresponds to the annealing temperature range of 200-550°C, respectively.

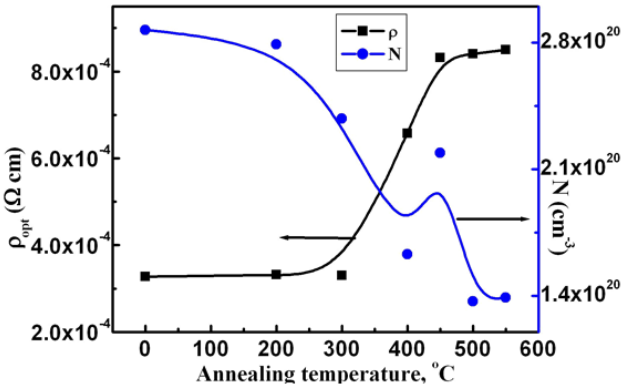

Fig.10 Dependence of optical resistivity (ρ_{opt}) and free carrier concentrations (N) of SnO_2 films on the annealing temperature.

4. Conclusion

SnO_2 thin films deposited onto a microscopic glass substrate by the e–beam evaporation method were annealed at different temperatures ranging from 200 to 550 °C in air in order to enhance the optical properties of these materials. The transmittance and reflectance spectra were used to determine the optical constants (n, k) of the SnO_2 film, and the effects of annealing temperature on the optical properties were investigated. The post thermal annealing is considered a significant tool to produce highly transparent and conduction SnO_2 films. With increasing the annealing temperature up to 500 °C, the optical gap records 3.65 eV. The optical constants decrease in the visible region with increasing the annealing temperature. The formed films become more homogenous at high annealing temperature. SnO_2 exhibits low thermal emissivity at temperature of 500 °C therefore these materials can be used in transparent heat mirror coatings applications. The optical resistivity of 3.32×10^{-4}-8.5×10^{-4} Ω cm which corresponds to the annealing temperature of 200-550°C were recorded in this study.

Acknowledgment

The authors would like to thank the Deanship of scientific research, King Saud University, Riyadh, Saudi Arabia, for funding and supporting this research.

References

[1] H. M. Alia, H. A. Mohamed and S. H. Mohamed, *Eur. Phys. J. Appl. Phys.* **31**, 87 (2005).

[2] M. Chen, Z. L. Pei, C. Sun, L.S. Wen and X. Wang, *J. Cryst. Growth* **220**, 254 (2000).

[3] B. Saha, R. Thapa and K. K. Chattopadhyay, *Solid State Commun.* **145**, 33 (2008).

[4] M. Kul, A. S. Aybek, E. Turan, M. Zor and S. Irmak, Sol. Energy Mater. *Sol. Cells* **91**, 1927 (2007).

[5] A. Nadarajah, M. E. Carnes, M. G. Kast, D. W. Johnson and S. W. Boettcher, *Chem. Mater.* To be published (2014).

[6] N. G. Deshpande, J. C. Vyas and R. Sharma, *Thin Solid Films* **516**, 8587 (2008).

[7] D. Miao, Q. Zhao, S. Wu, Z. Wang, X. Zhang and X. Zhao, *J. Non-Crystall. Solids* **356**, 2557 (2010).

[8] G. Brauer, J. Szczyrbowski and G. Teshner, *Surf. Coat. Technol.* **94-95**, 658 (1997).

[9] V. N. Zhitomirsky, T. David, R. L. Boxman, S. Goldsmith, A. Verdyan, Y. M. Soifer and L. Rapoport, *Thin Solid Films* **492**, 187 (2005).

[10] J. R. Brown, P. W. Haycock, L. M. Smith, A. C. Jones and E. W. Williams, *Sens. Actuators.* **B 63**, 109 (2000).

[11] S. Boycheva, A. K. Sytchkova, M. L. Grilli and A. Piegari, *Thin Solid Films* **515**, 8469 (2007).

[12] A. N. Banerjee, S. Kundoo, P. Saha and K. K. Chattopadhyay, *J. Sol-Gel Sci. Technol.* **28**, 105 (2003).

[13] W. Chen, D. Ghosh and S.W. Chen, *J. Mater. Sci.* **43**, 5291 (2008).

[14] J. H. Kim, K. A. Jeon, G. H. Kim and S.Y. Lee, *Appl. Surf. Sci.* **252**, 4834 (2006).

[15] J. J. Berry, D. S. Ginley and P.E. Burrows, *Appl. Phys. Lett.* **92**, 193304 (2008).

[16] M. Oshima and K. Yoshino, *J. Electron. Mater.* **39**, 816 (2010).

[17] M. A. Yıldırım, Y. Akaltun and A. Ates, *Solid State Sci.* **14**, 1282 (2012).

[18] A. F. Khan, M. Mehmood, M. Aslam and M. Ashraf, *Appl. Surf. Sci.* **256**, 2252 (2010).

[19] K. L. Chopra, S. Major and D. K. Pandya, *Thin Solid Films* **102**, 1 (1983).

[20] H. A. Mohamed, *J. Phys. D*: *Appl. Phys*. **40**, 4234 (2007).

[21] M. M. Hasan, A. S. M. A. Haseeb, R. Saidur and H. H. Masjuki, *Int. J. Chem. Biomol. Eng.* **1**, 93 (2008)

[22] J. Tauc, Amorphous and Liquid Semiconductors, (Plenum Press, New York, 1979).

[23] T. S. Moss, *Phys. Stat. Sol.* **B 131**, 415 (1985).

[24] Y. Akaltun, M. A. Yıldırım, A. Ates and M. Yıldırım, *Opt. Commun.* **284**, 2307 (2011).

[25] L. Hannachi and N. Bouarissa, *Physica* **B 404**, 3650 (2009).

[26] S.Y. Kim, *Appl. Opt.* **35**, 6703 (1996).

[27] E. Marquez, A. M. Bernal-Oliva, J. M. Gonzalez-Leal, R. Prieto-Alcon, A. Ledesma, R.

[28] Jimenez-Garay and I. Martil, Mater. *Chem. Phys.* **60**, 231 (1999).

[29] Z. Z. You and G. J. Hua, *Vacuum* **83**, 984 (2009).

[30] A. De, P. K. Biswas and J. Manara, *Mater. Charact.* **58**, 629 (2007)

[31] P. K. Biswas, A. De, N. C. Pramanika, P. K. Chakraborty, K. Ortner, V. Hock and S. Korder, *Mater. Lett.* **57**, 2326 (2003).

[32] M. S. Reddy, K.T. R. Reddy, B.S. Naidu and P.J. Reddy, *Opt. Mater.* **4**, 787 (1995).

[33] C. H. L. Weijtens and P. A. C. Van loon, *Thin Solid Films* **196**, l10 (1991).

[34] A. Mosbah and M. S. Aida, J. Alloy. *Compd* **515**,149 (2012).